

Duality of gauge field singularities and the structure of the flux tube in Abelian-projected SU(2) gauge theory and the dual Abelian Higgs model

Y. Koma* and M. Koma†

Max-Planck-Institut für Physik, Föhringer Ring 6, D-80805 München, Germany

E.-M. Ilgenfritz‡

Institut für Physik, Humboldt Universität zu Berlin, D-10115 Berlin, Germany

T. Suzuki§

*Institute for Theoretical Physics, Kanazawa University,
Kakuma-machi, Kanazawa, Ishikawa 920-1192, Japan*

M.I. Polikarpov¶

ITEP, B.Chermushkinskaya 25, RU-117259 Moscow, Russia

(Dated: February 8, 2020)

The structure of the flux-tube profile in Abelian-projected (AP) SU(2) gauge theory in the maximally Abelian gauge is studied. The connection between the AP flux tube and the classical flux-tube solution of the U(1) dual Abelian Higgs (DAH) model is clarified in terms of the path-integral duality transformation. This connection suggests that the electric photon and the magnetic monopole parts of the Abelian Wilson loop can act as separate sources creating the Coulombic and the solenoidal electric field inside a flux tube. The conjecture is confirmed by a lattice simulation which shows that the AP flux tube is composed of these two contributions.

I. INTRODUCTION

When the QCD vacuum is viewed as a *dual* superconductor [1, 2], the quark confinement mechanism can be immediately understood: the (color-) electric flux associated with a quark-antiquark ($q\bar{q}$) system is squeezed into an almost-one-dimensional flux tube by the *dual* Meissner effect caused by magnetic monopole condensation. This picture leads to a linear confinement potential and is a dual analogue of the magnetic Abrikosov vortex in an ordinary superconductor [3, 4, 5]. It is natural to expect that it can be quantitatively formulated by a dual version of an Abelian Higgs model, the dual Abelian Higgs (DAH) model. The Lagrangian – besides the kinetic terms of each field and a minimal coupling between the two fields – should contain a monopole self-interaction term that allows for a broken phase of dual gauge symmetry. The DAH model indeed has an electric flux-tube solution of the static $q\bar{q}$ system [5].

A linear potential emerging from a flux tube is quite welcome to give an interpretation for the area law behavior of the Wilson loop observed in lattice QCD simulations [6]. It would explain the Regge trajectory pattern or other string-like properties of hadrons [7]. Then the problem arises how to derive the dual superconductor scenario from QCD, that is, how to formally derive the DAH model from QCD. As a minimum, one would like to observe certain characteristic features of the dual superconductor, such as the formation of flux tubes, through a Monte-Carlo simulation of lattice QCD.

*ykoma@mppmu.mpg.de

†mkoma@mppmu.mpg.de

‡ilgenfri@physik.hu-berlin.de

§suzuki@hep.s.kanazawa-u.ac.jp

¶polykarp@heron.itep.ru

As for the formal derivation, it is known that if magnetic monopoles are introduced as the consequence of Abelian projection *à la* 't Hooft [8] and if the diagonal components of gluons play a dominant role (compared to the off-diagonal ones) in the long distance behavior of QCD (Abelian dominance), a condensed phase of monopoles is realized beyond a certain critical scale [9, 10]. Remarkably, lattice QCD simulations with non-Abelian configurations undergoing 't Hooft's Abelian-projection (typically in the maximally Abelian gauge, MAG) support this scenario numerically. For instance, the string tension measured by the “Abelian Wilson loop” constructed from the Abelian link variables (the “Abelian string tension”), is almost saturating the non-Abelian string tension [11]. In this context, applying the Zwanziger formalism [12], one can introduce the dual gauge field which is minimally coupled to monopoles. Summing over monopole current trajectories [13], one can also introduce a monopole field. This formulation finally leads to the DAH model [14, 15, 16, 17]. However, it is difficult to determine the effective couplings of the DAH model through this analytical derivation. In order to accomplish this, one needs numerical investigations of monopole dynamics on the lattice, for instance by means of the inverse Monte-Carlo method [18, 19, 20, 21].

Just in order to relate the flux-tube structures of the non-Abelian gauge theory and the DAH model, the profile of electric field and monopole current distribution induced by an Abelian Wilson loop have been studied within the Abelian-projection scheme [22, 23, 24, 25]. It has been found that the flux-tube structure is similar to the flux-tube solution in the DAH model. From now we call the former one “Abelian-projected (AP) flux tube” and the latter one “DAH flux tube”. We add here the remark that the connection between the AP flux tube and the DAH flux tube is not on equal footing because the former contains the quantum effects at work in non-Abelian lattice gauge simulations while the latter is just a classical solution obtained by solving the field equations. Having in mind this conceptual difference, the similarity of the corresponding flux profiles is quite suggestive, such that it makes sense to determine the couplings of the DAH model through the comparison between the two flux tubes [25, 26]. Once the DAH parameters are fixed in this way, one can use the DAH model as a starting point for further analyses of hadronic objects [27, 28, 29]. It will also be worth investigating the dynamics of the flux tube by deriving an effective string action from the DAH model [30, 31, 32, 33, 34, 35].

It is important to understand to what extent the AP flux tube can be related to the DAH flux tube. It is crucial to realize the “composed structure” of the AP flux tube. In fact, in the DAH model, as we explain later in detail, the appearance of the confining electric flux tube is due to the superposition of two well distinguished components, a Coulombic electric field directly induced by the electric charges and a solenoidal electric field induced by monopole supercurrent. Both correspond to the Coulombic and the linear rising part of the potential between colored particles. If such a structure is found for the AP flux tube, too, this will be an additional argument in favor of the DAH model description.

The guiding idea to discover this kind of structure of the AP flux-tube profile is inspired by the measurement of the q - \bar{q} potential in terms of the Abelian Wilson loop. The investigation of the Abelian Wilson loop using the decomposition into an electric photon part (“photon Wilson loop”) and a magnetic monopole part (“monopole Wilson loop”) shows that the Abelian potential consists of a Coulombic and a linear potential [36, 37, 38]. We notice that this structure is quite similar to the q - \bar{q} potential in the DAH model.

In this paper, we present the results of measurement of the AP flux-tube profiles, induced by the photon and the monopole Wilson loops within the AP-SU(2) lattice gauge theory in the MAG. In section II, we outline the derivation of the U(1) DAH model by performing the path-integral duality transformation starting from a Villain type compact

QED viewed as the approximate action of the AP gauge theory. Throughout the derivation, we pay attention to the problem how the *magnetic* Dirac strings in the AP gauge field are transformed, and how the *electric* Dirac string emerges in the dual gauge field in the presence of external electric current (quark sources). In section III, we show that the electric Dirac string plays an important role in the formation of the flux tube in the DAH model. In section IV we explain the connection between the photon and the monopole Wilson loops in the AP-SU(2) gauge theory. The profile of the DAH flux tube provides support for this idea. Section V is the summary.

II. PATH-INTEGRAL DUALITY TRANSFORMATION

From lattice studies of the effective monopole action in the MAG [18, 19, 20, 21], it is numerically suggested that, at some infrared scale, the partition function of the AP-SU(2) theory is represented by the following Villain type modification of compact QED

$$\mathcal{Z} = \int_{-\pi}^{\pi} \mathcal{D}\theta \sum_{n^{(m)} \in \mathbb{Z}} \exp \left[-\frac{1}{2} (F, \Delta D F) + i(\theta, j) \right], \quad (2.1)$$

where $F(C_2)$ is the field strength

$$F = d\theta - 2\pi n^{(m)}, \quad (2.2)$$

which is composed of compact link variables, $\theta(C_1) \in [-\pi, \pi)$, and magnetic Dirac strings, $n^{(m)}(C_2) \in \mathbb{Z}$. θ corresponds to the Abelian gauge field. The operator D is a general differential operator and Δ is the Laplacian on the lattice. In the infrared limit, the operator D is numerically shown to be well-described by the following form: $D = \beta_e \Delta^{-1} + \alpha + \gamma \Delta$, where β_e , α and γ are renormalized coupling constants of the monopole action which satisfy the relation $\beta_e \gg \alpha, \gamma$ [39]. An external electric current is denoted by $j(C_1) \in \mathbb{Z}$, which interacts with θ . For a closed electric current, one may call the operator $W_A[j] = \exp[i(\theta, j)]$ the Abelian Wilson loop. The (inverse) effective gauge coupling is $\beta_e \equiv 4/e^2$. The action in (2.1) is invariant under U(1) gauge transformations $\theta \mapsto \theta + df$ generated by a phase $f(C_0)$, since $d^2 f = 0$, and $(df, j) = (f, \delta j) = 0$ as long as the external current is conserved, $\delta j = 0$. Due to the presence of magnetic Dirac string $n^{(m)}$, the Abelian Bianchi identity is now violated as

$$dF = -2\pi dn^{(m)} = 2\pi k, \quad (2.3)$$

where $dn^{(m)} = -k$. The magnetic Dirac strings are bordered by magnetic monopole currents $k(C_3)$, which are conserved as well, $dk = 0$.

Now, we consider the path-integral duality transformation of the partition function (2.1). Concerning the summation over the magnetic Dirac strings, we can refer to Poincaré's lemma. These strings are divided into a sum of open strings, $p(C_2) \in \mathbb{Z}$ spanned by the monopole currents, and closed string fluctuations, dq (where $q(C_1) \in \mathbb{Z}$), as

$$n^{(m)} = p + dq, \quad (2.4)$$

satisfying

$$dp = -k, \quad d^2 q = 0. \quad (2.5)$$

The summation is then replaced by independent summation over k (with constraint $dk = 0$) and q [40]

$$\sum_{n^{(m)} \in \mathbb{Z}} = \sum_{k \in \mathbb{Z}, dk=0} \sum_{q \in \mathbb{Z}}. \quad (2.6)$$

For simplicity, we approximate the differential operator in Eq. (2.1) to the leading term, $D = \beta_e \Delta^{-1}$. We make the electric-photon and magnetic-monopole parts of θ explicit by applying the Hodge decomposition as

$$\theta = \Delta^{-1} \Delta \theta = \Delta^{-1} (\delta d + d \delta) \theta = \theta^{ph} + \theta^{mo} + 2\pi q + \Delta^{-1} d \delta (\theta - 2\pi q), \quad (2.7)$$

where

$$\theta^{ph} \equiv \Delta^{-1} \delta F = \theta - 2\pi q - \theta^{mo} - \Delta^{-1} d \delta (\theta - 2\pi q), \quad (2.8)$$

$$\theta^{mo} \equiv 2\pi \Delta^{-1} \delta p, \quad (2.9)$$

are the electric-photon (θ^{ph}) and the magnetic-monopole (θ^{mo}) parts of the Abelian gauge field. Note that the last equality in Eq. (2.7) is due to $d\theta = F + 2\pi n^{(m)}$. Δ^{-1} is the inverse of the lattice Laplacian Δ , corresponding to the Coulomb propagator. Now, θ^{ph} represent noncompact link variables. In fact, from Eq. (2.6) one finds that the integration over θ and the summation over q are to be replaced by

$$\int_{-\pi}^{\pi} \mathcal{D}\theta \sum_{q \in \mathbb{Z}} = \int_{-\infty}^{\infty} \mathcal{D}\theta^{ph}. \quad (2.10)$$

The last term in Eq. (2.8), a subject of gauge fixing, does not affect the further evaluation. Acting with an exterior derivative on θ^{mo} , one finds $d\theta^{mo} = 2\pi(n^{(m)} + C^{(m)} - dq)$ with $C^{(m)} = \Delta^{-1} \delta k$. Thus, the partition function is written as noncompact QED with explicit monopoles,

$$\mathcal{Z} = \int_{-\infty}^{\infty} \mathcal{D}\theta^{ph} \sum_{k \in \mathbb{Z}, dk=0} \exp \left[-\frac{\beta_e}{2} (d\theta^{ph} + 2\pi C^{(m)})^2 + i(\theta^{ph} + \theta^{mo}, j) \right]. \quad (2.11)$$

In this expression, of course, one realizes again the violation of Abelian Bianchi identity in the form

$$dF \equiv d(d\theta^{ph} + 2\pi C^{(m)}) = 2\pi dC^{(m)} = 2\pi k, \quad (2.12)$$

due to $dC^{(m)} = k$. We will call $W_{Ph}[j] = \exp[i(\theta^{ph}, j)]$ and $W_{Mo}[j] = \exp[i(\theta^{mo}, j)]$ the electric-photon Wilson loop and the magnetic-monopole Wilson loop, respectively.

Using the relation $(d\theta^{ph}, C^{(m)}) = (\theta^{ph}, \delta C^{(m)}) = 0$ (since $\delta C^{(m)} = 0$) we can write $(F)^2 = (d\theta^{ph})^2 + 4\pi^2 (C^{(m)})^2$. Imposing the gauge fixing condition $\delta\theta^{ph} = 0$, one can integrate over θ^{ph} . This yields a direct interaction term between electric currents j via the Coulomb propagator Δ^{-1} . Thus we have

$$\mathcal{Z} = \sum_{k \in \mathbb{Z}, dk=0} \exp \left[-\frac{1}{2\beta_e} (j, \Delta^{-1} j) - 2\pi^2 \beta_e (C^{(m)})^2 + i(\theta^{mo}, j) \right]. \quad (2.13)$$

Defining $C^{(e)}(*C_2) \equiv \Delta^{-1} \delta * j$ in analogy to $C^{(m)}$, the first term of the action can also be written in the form

$$\frac{1}{2\beta_e} (j, \Delta^{-1} j) = \frac{1}{2\beta_e} (*j, \Delta^{-1} *j) = \frac{1}{2\beta_e} (C^{(e)})^2 = 2\pi^2 \beta_m (C^{(e)})^2, \quad (2.14)$$

where we have introduced the (inverse) dual gauge coupling $\beta_m = 1/g^2$, which should satisfy $4\pi^2 \beta_e \beta_m = 1$ (*i.e.* $eg = 4\pi$).

Similarly, the square of $C^{(m)}$ can be rewritten

$$2\pi^2 \beta_e (C^{(m)})^2 = \frac{1}{2\beta_g} (k, \Delta^{-1} k) = \frac{1}{2\beta_g} (*k, \Delta^{-1} *k). \quad (2.15)$$

The exponential of this expression can further be understood as a functional integral over the magnetic part of a noncompact *dual* gauge field $\tilde{\theta}^{mo}(*C_1)$, minimally coupled to the magnetic monopole current,

$$\exp \left[-\frac{1}{2\beta_g} (*k, \Delta^{-1} *k) \right] = \int_{-\infty}^{\infty} \mathcal{D}\tilde{\theta}^{mo} \exp \left[-\frac{\beta_g}{2} (d\tilde{\theta}^{mo})^2 + i(\tilde{\theta}^{mo}, *k) \right]. \quad (2.16)$$

We have attached the superscript “ mo ” in order to distinguish it from the photon part of the dual gauge field, $\tilde{\theta}^{ph}(*C_1)$, which is defined in analogy to θ^{mo} in Eq. (2.9) as

$$\tilde{\theta}^{ph} = 2\pi\Delta^{-1}\delta n^{(e)}. \quad (2.17)$$

Here $n^{(e)}(*C_2) \in \mathbb{Z}$ denotes electric Dirac strings, satisfying $dn^{(e)} = -*j$. This field appears when we evaluate the monopole Wilson loop, due to the relation

$$(\theta^{mo}, j) - (\tilde{\theta}^{ph}, *k) = -2\pi(p, *n^{(e)}) = 2\pi N \quad (N \in \mathbb{Z}). \quad (2.18)$$

The direct coupling of j and k to θ^{mo} and $\tilde{\theta}^{ph}$, respectively, can be understood as an intersection term between electric and magnetic Dirac strings. As long as the Dirac quantization condition is satisfied, $eg = 4\pi$, this intersection term is quantized such as not to contribute to the functional integral ($\exp[i(2\pi N)] = 1$).

Collecting all terms, the partition function is found to be

$$\mathcal{Z} = \int_{-\infty}^{\infty} \mathcal{D}\tilde{\theta}^{mo} \sum_{k \in \mathbb{Z}, dk=0} \exp \left[-\frac{\beta_m}{2} (d\tilde{\theta}^{mo} + 2\pi C^{(e)})^2 + i(\tilde{\theta}^{mo} + \tilde{\theta}^{ph}, *k) \right]. \quad (2.19)$$

The action is invariant under the transformation $\tilde{\theta}^{mo} \mapsto \tilde{\theta}^{mo} + d\tilde{f}$. This is nothing but the realization of the dual gauge symmetry, which is closely related to the conserved magnetic monopole currents, $dk = 0$. In this action, the electric currents are now implicitly defined via the violation of the *dual* Abelian Bianchi identity written down for the dual field strength

$$\tilde{F} = d\tilde{\theta}^{mo} + 2\pi C^{(e)} \quad (2.20)$$

as

$$d\tilde{F} = 2\pi dC^{(e)} = 2\pi *j, \quad (2.21)$$

where $dC^{(e)} = *j$. If one defines the *full* dual gauge field $\tilde{\theta}$ as

$$\tilde{\theta} \equiv \tilde{\theta}^{mo} + \tilde{\theta}^{ph}, \quad (2.22)$$

the dual field strength can also be written as $\tilde{F} = d\tilde{\theta} - 2\pi n^{(e)}$. The violation of the dual Abelian Bianchi identity is then re-expressed as

$$d\tilde{F} = d(d\tilde{\theta} - 2\pi n^{(e)}) = -2\pi dn^{(e)} = 2\pi *j. \quad (2.23)$$

The transformed partition function is already in a form suggesting the dual Abelian Higgs (DAH) model. In order to finally arrive at the DAH model, we need to introduce a complex-scalar (monopole) field χ . This is equivalent to summing over monopole currents, however with a slightly more complicated form of the monopole action. We assume here that the resulting action will maintain the dual gauge symmetry, which is broken spontaneously. This means that the monopole field should minimally couple to the dual gauge field. Thus, the leading terms of the local action of the DAH model will be given by

$$S_{\text{DAH}} = \frac{\beta_m}{2} (\tilde{F})^2 + |(d + i\tilde{\theta})\chi|^2 + V(|\chi|^2). \quad (2.24)$$

The action is still invariant under U(1) dual gauge transformations

$$\chi \mapsto \chi \exp(i\tilde{f}), \quad \chi^* \mapsto \chi^* \exp(-i\tilde{f}), \quad \tilde{\theta} \mapsto \tilde{\theta} - d\tilde{f}. \quad (2.25)$$

For the potential term of the monopole field we adopt the simple form $V(|\chi|^2) = \lambda(|\chi|^2 - v^2)^2$ in order to open the possibility to have the monopole field condensed, where λ and v denote the strength of self-coupling and the tree-level monopole condensate.

III. STRUCTURE OF CLASSICAL FLUX-TUBE SOLUTION IN THE DAH MODEL

In this section we study the classical flux-tube solutions in a *continuum* DAH model which corresponds to the noncompact *lattice* DAH model, the derivation of which has been outlined in the last section.

The action of this continuum model is

$$S_{\text{DAH}} = \int d^4x \left[\frac{\beta_m}{2} \tilde{F}_{\mu\nu}^2 + |(\partial_\mu + i(B_\mu^{mo} + B_\mu^{ph}))\chi|^2 + \lambda(|\chi|^2 - v^2)^2 \right], \quad (3.1)$$

where the dual field strength is defined as

$$\tilde{F}_{\mu\nu} = \partial_\mu B_\nu^{mo} - \partial_\nu B_\mu^{mo} + 2\pi C_{\mu\nu}^{(e)}, \quad (3.2)$$

and we look for static solutions of minimal energy. We note that B_μ^{mo} is the continuum form of the regular dual gauge field denoted $\tilde{\theta}^{mo}$ on the lattice, B_μ^{ph} the continuum form of the singular dual gauge field $\tilde{\theta}^{ph}$ and $C_{\mu\nu}^{(e)}$ corresponds to $C^{(e)}(*C_2)$. The DAH model with an electric Dirac string, which is included in B_μ^{ph} , has classical solutions which correspond to *open* flux tubes. These solutions are obtained by solving the field equations taking into account certain boundary conditions associated with the string singularity.

Inserting the polar decomposition of the monopole field $\chi = \phi \exp(i\eta)$ ($\phi, \eta \in \Re$), the field equations for B_μ^{mo} and ϕ are written as

$$\beta_m \partial_\mu (\partial_\mu B_\nu^{mo} - \partial_\nu B_\mu^{mo} + 2\pi C_{\mu\nu}^{(e)}) = 2(B_\nu^{mo} + B_\nu^{ph})\phi^2 = k_\nu, \quad (3.3)$$

$$(\partial_\mu \phi)^2 + (B_\mu^{mo} + B_\mu^{ph})^2 \phi = 2\lambda\phi(\phi^2 - v^2), \quad (3.4)$$

where

$$C_{\mu\nu}^{(e)}(x) = \frac{1}{4\pi^2} \int d^4y \frac{1}{|x-y|^2} *(\partial \wedge j(y))_{\mu\nu}. \quad (3.5)$$

Note that we can drop $C_{\mu\nu}^{(e)}$ from the field equation (3.3) since $\partial_\mu C_{\mu\nu}^{(e)} = 0$. In these equations, the phase η has been absorbed into the definition of B_μ^{mo} .

Let us now consider a $q\bar{q}$ system that each electric charge is placed at $\mathbf{x}_1 = (-r/2)\mathbf{e}_z$, and $\mathbf{x}_2 = (+r/2)\mathbf{e}_z$, respectively. The distance is r . The corresponding electric current is written as $j_\mu(x) = \delta_{\mu 0}(\delta(\mathbf{x} - \mathbf{x}_1) - \delta(\mathbf{x} - \mathbf{x}_2))$. This system will have cylindrical geometry, so that all field variables can be described in cylindrical coordinates (ρ, φ, z) , where ρ denotes the radial coordinate and φ the azimuthal angle around the z axis. The fields can be parametrized as

$$\phi = \phi(\rho, z), \quad (3.6)$$

$$\mathbf{B}^{mo} = B^{mo}(\rho, z)\mathbf{e}_\varphi \equiv \frac{\hat{B}^{mo}(\rho, z)}{\rho}\mathbf{e}_\varphi, \quad (3.7)$$

$$\mathbf{B}^{ph} = -\frac{n}{2\rho} \left(\frac{z+r/2}{\sqrt{\rho^2 + (z+r/2)^2}} - \frac{z-r/2}{\sqrt{\rho^2 + (z-r/2)^2}} \right) \mathbf{e}_\varphi, \quad (3.8)$$

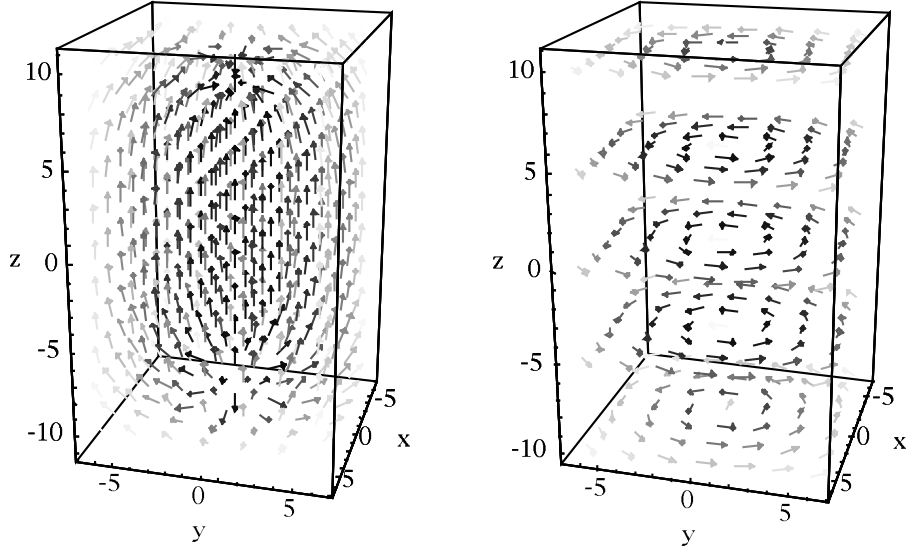


FIG. 1: Profiles of electric field \mathbf{E}/a^2 (left) and monopole current \mathbf{k}/a^3 (right) in the DAH model, where a denotes a certain length scale.

where the factor n in \mathbf{B}^{ph} is the winding number of the flux tube (an integer value), which is determined by the representation of the electric charges [41, 42, 43]. The fundamental representation corresponds to $n = 1$.

The field equations (3.3) and (3.4) are then reduced to:

$$\beta_m \left(\frac{\partial^2 \hat{B}^{mo}}{\partial \rho^2} - \frac{1}{\rho} \frac{\partial \hat{B}^{mo}}{\partial \rho} + \frac{\partial^2 \hat{B}^{mo}}{\partial z^2} \right) - 2 \left(\hat{B}^{mo} - \frac{n}{2} \left(\frac{z+r/2}{\sqrt{\rho^2 + (z+r/2)^2}} - \frac{z-r/2}{\sqrt{\rho^2 + (z-r/2)^2}} \right) \right) \phi^2 = 0, \quad (3.9)$$

$$\frac{\partial^2 \phi}{\partial \rho^2} + \frac{1}{\rho} \frac{\partial \phi}{\partial \rho} + \frac{\partial^2 \phi}{\partial z^2} - \left(\frac{\hat{B}^{mo} - \frac{n}{2} \left(\frac{z+r/2}{\sqrt{\rho^2 + (z+r/2)^2}} - \frac{z-r/2}{\sqrt{\rho^2 + (z-r/2)^2}} \right)}{\rho} \right)^2 \phi - 2\lambda\phi(\phi^2 - v^2) = 0. \quad (3.10)$$

The boundary conditions are specified so as to make the energy of the system finite as

$$\hat{B}^{mo} = 0 \text{ as } \rho \rightarrow 0, \text{ and } \phi = 0 \text{ as } \rho \rightarrow 0 \text{ for } -r \leq z \leq r, \\ \hat{B}^{mo} = \frac{n}{2} \left(\frac{z+r/2}{\sqrt{\rho^2 + (z+r/2)^2}} - \frac{z-r/2}{\sqrt{\rho^2 + (z-r/2)^2}} \right) \text{ and } \phi = v \text{ as } \rho, z \rightarrow \infty. \quad (3.11)$$

After getting the numerical solution of the field equations for \hat{B}^{mo} and ϕ , the profiles of the electric field are computed as

$$\mathbf{E} = \nabla \times \mathbf{B}^{mo} + 2\pi \mathbf{C}^{(e)} \equiv \mathbf{E}^{mo} + \mathbf{E}^{ph}, \quad (3.12)$$

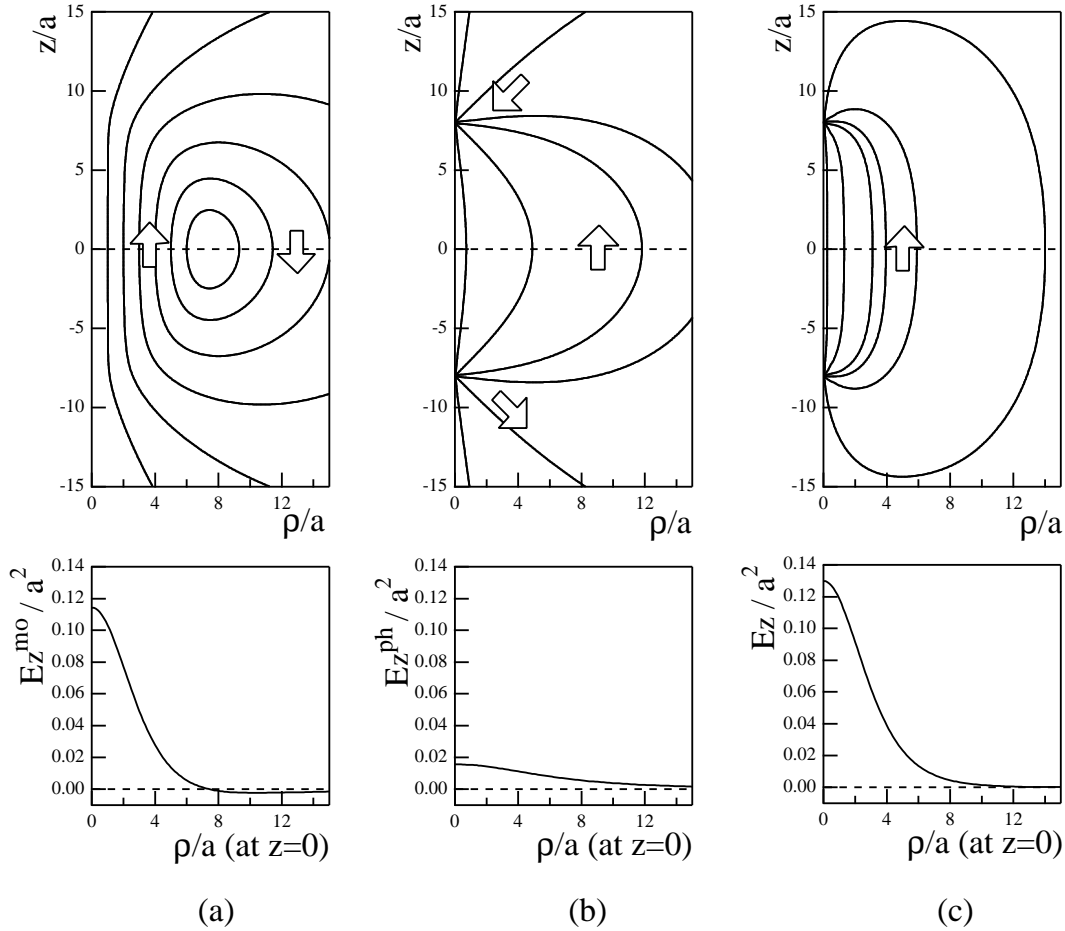


FIG. 2: The flux-line pattern of the electric field (upper row) and the electric field strength as a function of the cylindrical radius (lower row): (a) the solenoidal electric field \mathbf{E}^{mo} and (b) the Coulombic field \mathbf{E}^{ph} add up to the flux-tube profile of the full electric field (c).

where

$$\mathbf{E}^{mo} = -\frac{1}{\rho} \frac{\partial \hat{B}^{mo}}{\partial z} \mathbf{e}_\rho + \frac{1}{\rho} \frac{\partial \hat{B}^{mo}}{\partial \rho} \mathbf{e}_z, \quad (3.13)$$

$$\begin{aligned} \mathbf{E}^{ph} = & \frac{n}{2} \left(\frac{\rho}{(\rho^2 + (z+r/2)^2)^{3/2}} - \frac{\rho}{(\rho^2 + (z-r/2)^2)^{3/2}} \right) \mathbf{e}_\rho \\ & + \frac{n}{2} \left(\frac{z+r/2}{(\rho^2 + (z+r/2)^2)^{3/2}} - \frac{z-r/2}{(\rho^2 + (z-r/2)^2)^{3/2}} \right) \mathbf{e}_z. \end{aligned} \quad (3.14)$$

The profile of the monopole current is given by

$$\begin{aligned} \mathbf{k} &= 2(\mathbf{B}^{mo} + \mathbf{B}^{ph}) \phi^2 \\ &= 2 \left(\hat{B}^{mo} - \frac{n}{2} \left(\frac{z+r/2}{\sqrt{\rho^2 + (z+r/2)^2}} - \frac{z-r/2}{\sqrt{\rho^2 + (z-r/2)^2}} \right) \right) \phi^2 \mathbf{e}_\varphi. \end{aligned} \quad (3.15)$$

In Figs. 1 and 2 we show such profiles for parameters $\beta_m = 1/g^2 = 1$, $m_B/a = \sqrt{2}gv/a = 0.5$ and $m_\chi = 2\sqrt{\lambda}v/a = 0.5$, taking the q - \bar{q} separation $r = 16a$. Here a is a certain length scale. Although the electric field derived from the magnetic part of the dual gauge field, \mathbf{E}^{mo} , takes positive value near the center, it turns *negative* beyond a certain radius ρ_c (in the given case, $\rho \sim 7a$). This signals the appearance of a *solenoidal* electric field. We find that this

plays a role to cancel the Coulombic field, \mathbf{E}^{ph} , induced by electric charges, at some distance from the electric Dirac string. It is then avoided that the total electric field penetrates too far into the dual-superconducting vacuum. By superposition the full electric field acquires finally the form of a flux tube. Note that the solenoidal electric field exists entirely due to the presence of the azimuthal monopole supercurrent \mathbf{k} .

It is usually taken for granted that the classical flux-tube solution has perfect translational invariance along the q - \bar{q} direction. Here we would like to mention that this is not true for a *finite length* q - \bar{q} system where the flux tube consists of the Coulombic and the solenoidal parts. The former component of the field clearly does not possess such translational invariance, and the latter one has a shape to cancel the Coulombic field at $\rho \rightarrow \infty$. In order to have translational invariance, we would need practically infinite q - \bar{q} separation, $r \rightarrow \infty$, where the contribution from \mathbf{E}^{ph} completely disappears and only the profile from \mathbf{E}^{mo} remains.

IV. FLUX-TUBE PROFILE FROM LATTICE SIMULATION

Now let us consider the role of θ^{ph} and θ^{mo} for the DAH model and for the resulting flux-tube solution. As seen from the path-integral duality transformation, which has led us to the DAH model, we find that a photon Wilson loop $W_{Ph}[j] = \exp[i(\theta^{ph}, j)]$ leads to the square of the Coulombic field strength $C^{(e)}$ after the functional integration over θ^{ph} , while a monopole Wilson loop $W_{Mo}[j] = \exp[i(\theta^{mo}, j)]$ is translated into an interaction term between $\tilde{\theta}^{ph}$ and the monopole field. In other words, without a photon Wilson loop we could not see the Coulombic electric field originating from the quark charge in the DAH model. On the other hand, without a monopole Wilson loop we could not have an electric part, $\tilde{\theta}^{ph}$, after the duality transformation. We should remind that this contribution is really important for the determination of the boundary condition of the behavior of the dual gauge field, $\tilde{\theta}^{mo}$, which induces a monopole supercurrent and the resulting solenoidal electric-field profile.

Hence, we conclude that the photon Wilson loop is the appropriate source to create the Coulombic electric field, while the monopole Wilson loop is the source for the solenoidal electric field in the DAH model. The considerations above suggest how to observe it on the lattice. As it has been studied in Refs. [22, 23, 24, 25], the flux-tube profile can be measured by Monte-Carlo simulation of AP *lattice* gauge theory. The main idea adopted in these simulations is to measure the expectation value of a local operator \mathcal{O} in the vacuum with an Abelian Wilson loop, $W_A[j] = \exp[i(\theta, j)]$, inserted as an external source. To measure such a quantity, one can use the following relation:

$$\begin{aligned} \langle \mathcal{O} \rangle_j &= \frac{\int_{-\pi}^{\pi} \mathcal{D}\theta \sum_{n^{(m)} \in \mathbb{Z}} \mathcal{O} \exp \left[-\frac{\beta_e}{2} (d\theta - 2\pi n^{(m)})^2 + i(\theta, j) \right]}{\int_{-\pi}^{\pi} \mathcal{D}\theta \sum_{n^{(m)} \in \mathbb{Z}} \exp \left[-\frac{\beta_e}{2} (d\theta - 2\pi n^{(m)})^2 + i(\theta, j) \right]} \\ &= \frac{\int_{-\pi}^{\pi} \mathcal{D}\theta \sum_{n^{(m)} \in \mathbb{Z}} \mathcal{O} W_A[j] \exp \left[-\frac{\beta_e}{2} (d\theta - 2\pi n^{(m)})^2 \right]}{\int_{-\pi}^{\pi} \mathcal{D}\theta \sum_{n^{(m)} \in \mathbb{Z}} W_A[j] \exp \left[-\frac{\beta_e}{2} (d\theta - 2\pi n^{(m)})^2 \right]} \\ &= \frac{\langle \mathcal{O} W_A[j] \rangle_0}{\langle W_A[j] \rangle_0}, \end{aligned} \tag{4.1}$$

where $\langle \cdots \rangle_j$ denotes an average in the vacuum with an external source, and $\langle \cdots \rangle_0$ an average in the vacuum without external source. Thus by measurement of the expectation values of $\langle \mathcal{O} W_A \rangle_0$ and the Abelian Wilson loop $\langle W_A \rangle_0$, the expectation value of a local operator associated with the external source, $\langle \mathcal{O} \rangle_j$, can be evaluated. Below, the Abelian field strength F and the monopole current k have been chosen as local operators \mathcal{O} . The simulations are *not* done in the *reduced* AP gauge theory but in the non-Abelian theory, with configurations having undergone Abelian

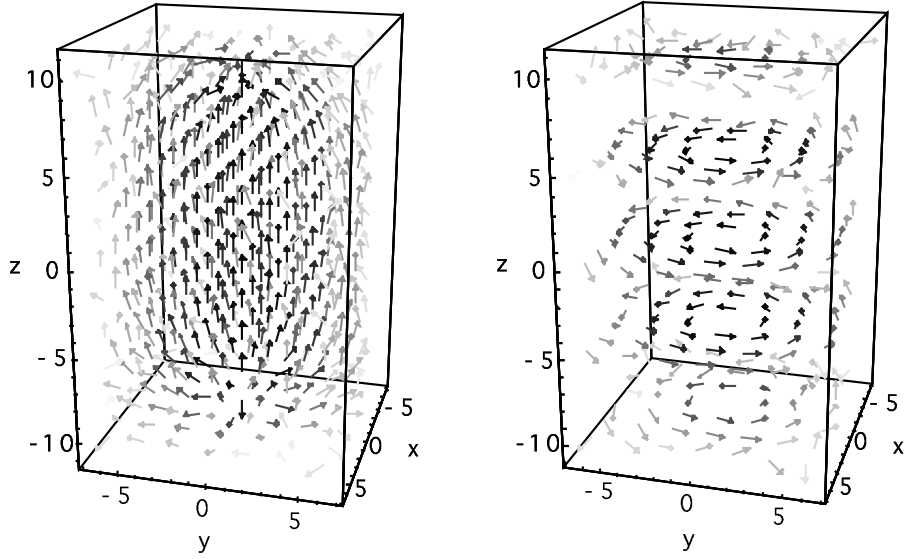


FIG. 3: Profiles of electric field (left) and monopole current (right) at $\beta = 2.5115$, with an Abelian Wilson loop of size 16×4 on a 32^4 lattice.

projection. The MAG fixing and Abelian projection reduce the degrees of freedom to those figuring in the AP gauge theory which we have approximated by (2.1). Typical profiles of the electric field and monopole current evaluated in this context are shown in Fig. 3 (details of the simulation are given in Appendix A). At glance, the shape of the resulting profiles are very similar to the flux-tube profiles obtained within the DAH model, see Fig. 1.

Next, we extend these studies to the case of the photon Wilson loop and the monopole Wilson loop as the source. We remind that due to Eq. (2.7) the Abelian Wilson loop can be decomposed into a photon and a monopole Wilson loop

$$W_A[j] = W_{Ph}[j] \cdot W_{Mo}[j]. \quad (4.2)$$

First, let us consider the expectation value of the Abelian field strength. The corresponding field strength operator can be written as

$$F = d\theta^{ph} + 2\pi C^{(m)} \equiv F_{Ph} + F_{Mo}. \quad (4.3)$$

Eq. (4.1) requires now to evaluate the quantum averages in the numerator and the denominator as follows

$$\langle F \rangle_j = \frac{\langle (F_{Ph} + F_{Mo}) W_{Ph}[j] W_{Mo}[j] \rangle_0}{\langle W_{Ph}[j] W_{Mo}[j] \rangle_0} \approx \frac{\langle F_{Ph} W_{Ph}[j] \rangle_0}{\langle W_{Ph}[j] \rangle_0} + \frac{\langle F_{Mo} W_{Mo}[j] \rangle_0}{\langle W_{Mo}[j] \rangle_0} = \langle F_{Ph} \rangle_j + \langle F_{Mo} \rangle_j. \quad (4.4)$$

Here, to get the second, *approximate* equality, we have assumed factorization of vacuum expectation values of operators X_{Ph} and Y_{Mo} , defined in terms of the photon part and the monopole part of the Abelian gauge field θ , respectively, $\langle X_{Ph} Y_{Mo} \rangle_0 \approx \langle X_{Ph} \rangle_0 \langle Y_{Mo} \rangle_0$. This factorization property is indeed observed in many lattice simulations in the MAG [36, 37, 38, 44]. For instance, the q - \bar{q} potential from the Abelian Wilson loop shows the behavior

$$V_A(r) = - \lim_{T \rightarrow \infty} \frac{1}{T} \ln \langle W_A[j] \rangle_0 \approx - \lim_{T \rightarrow \infty} \frac{1}{T} [\ln \langle W_{Ph}[j] \rangle_0 + \ln \langle W_{Mo}[j] \rangle_0] = V_{Ph}(r) + V_{Mo}(r). \quad (4.5)$$

It has been shown that the potential from the photon and monopole parts asymptotically behaves as $V_{Ph}(r) \propto 1/r$ and $V_{Mo}(r) \propto r$, respectively. This means that the linear rising confinement potential is created by the monopole

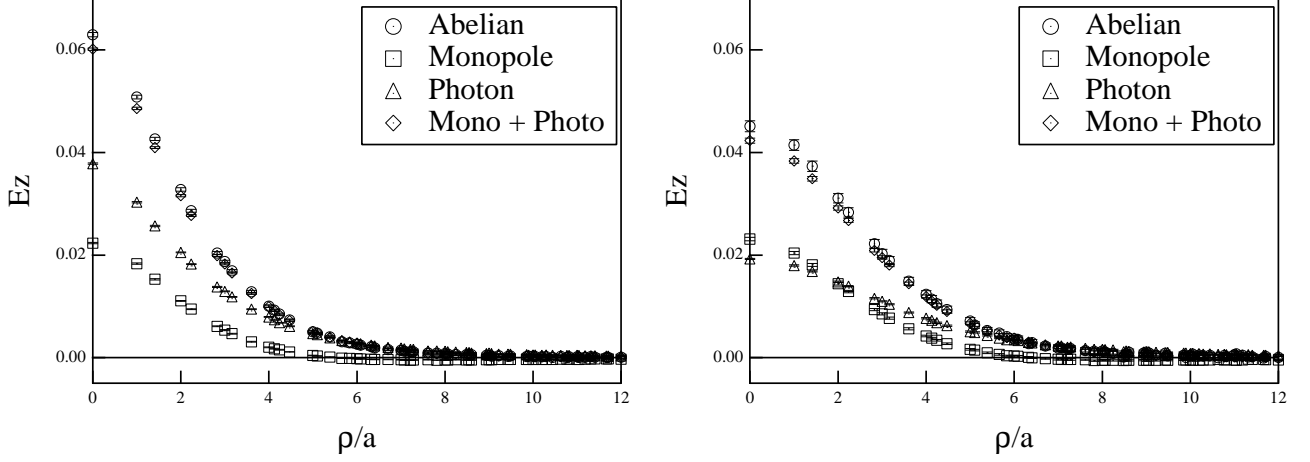


FIG. 4: Electric field profile from correlators with Abelian, photon and monopole Wilson loops at $r = 6a = 0.49$ fm (left) and at $r = 12a = 0.97$ fm (right).

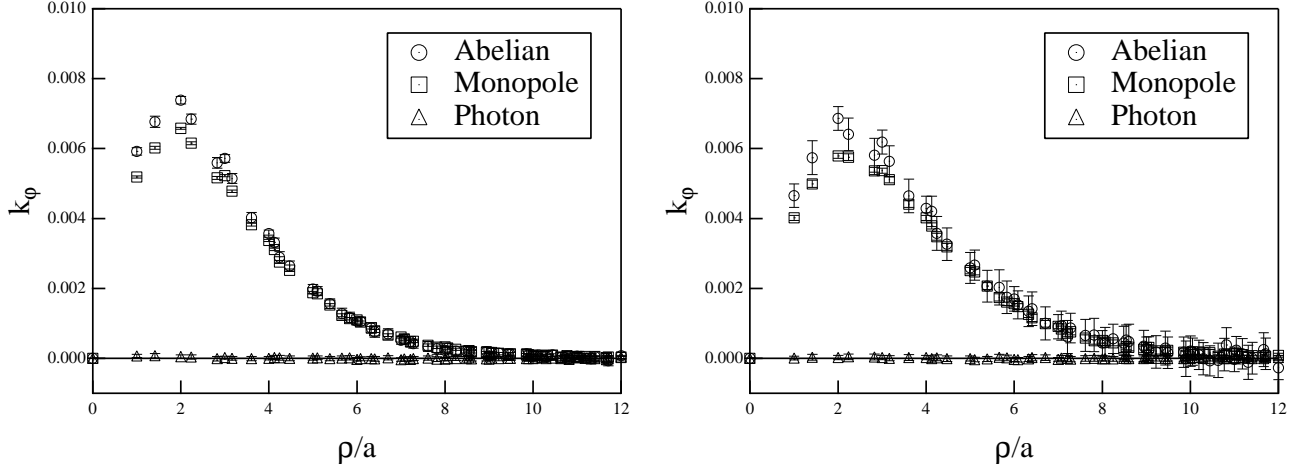


FIG. 5: Monopole current profile from correlators with Abelian, photon and monopole Wilson loops at $r = 6a = 0.49$ fm (left) and at $r = 12a = 0.97$ fm (right).

part. Note that almost the full string tension corresponding to the Abelian Wilson loop is due to the monopole part [36, 37, 38]. Relation (4.4) suggests that in the AP lattice simulations one should be able to separate the flux-tube profile in a way similar to that shown in Fig. 2 for the DAH model. One would expect that the actual flux tube appears if we superimpose the Coulombic and the induced solenoidal electric field. This picture would be finally also consistent with the behavior of the q - \bar{q} potential extracted from Wilson loops.

Second, we consider the expectation value of the monopole current k . Since we have the obvious relation

$$k = -\frac{1}{2\pi}dF = -dC^{(m)} = k_{Mo}, \quad (4.6)$$

while the photon part of the monopole current vanishes, $k_{Ph} \propto d^2\theta^{ph} = 0$, we will get

$$\langle k \rangle_j \approx \frac{\langle k_{Mo} W_{Mo}[j] \rangle_0}{\langle W_{Mo}[j] \rangle_0} = \langle k_{Mo} \rangle_j. \quad (4.7)$$

This means that the correlator of the monopole current only with the monopole Wilson loop will account for the full

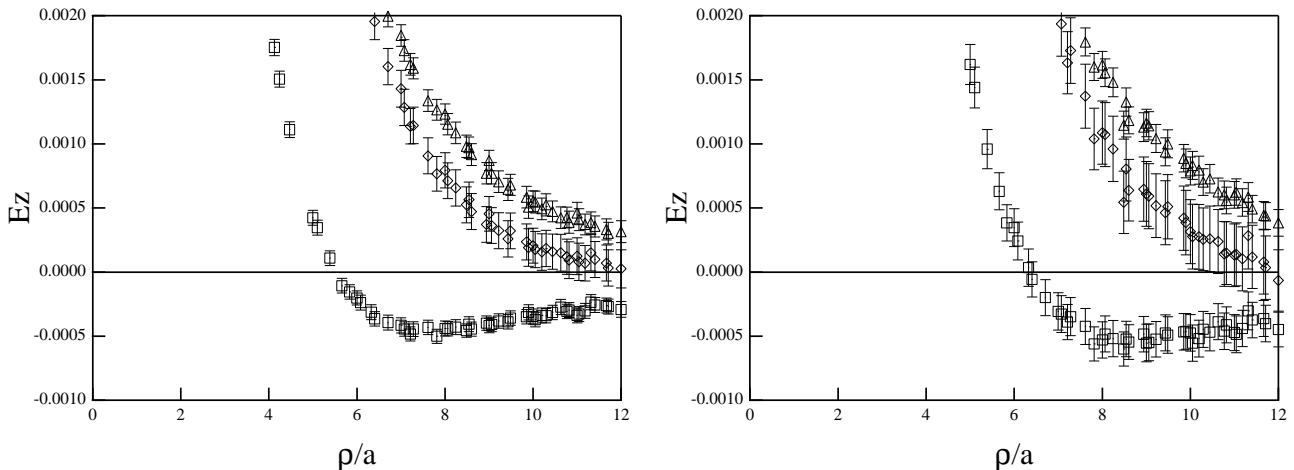


FIG. 6: The same plots as in Fig. 4, for flux tubes of length $r = 0.49$ fm and $r = 0.97$ fm, with the E_z axis rescaled. The profile directly from the Abelian Wilson loop is omitted.

expectation value of monopole current and, at the same time, the correlator with the photon Wilson loop vanishes everywhere.

In Figs. 4 and 5 we show the lattice flux-tube profiles calculated using the complete Abelian, the photon, and the monopole Wilson loops. The measurement has been done at $\beta = 2.5115$ on a 32^4 lattice after the MAG has been fixed. The q - \bar{q} distances are $r = 6a$ and $12a$. The lattice spacing is $a = 0.081$ fm, which has been determined from the non-Abelian string tension σ_L , $\sqrt{\sigma_{phys}} = \sqrt{\sigma_L}/a \equiv 440$ MeV. Physically, the q - \bar{q} distances correspond to 0.49 fm and 0.97 fm, respectively (see, Appendix A). In Fig. 6 we show the same electric field profiles as in Fig. 4, focussing on the region where $E_z \sim 0$. We see that these lattice results concerning the behavior of the profiles strongly support our considerations above; from the photon and the monopole Wilson loops we obtain the Coulombic electric field and the solenoidal electric field with the monopole supercurrent profile, respectively. We find that the sum of these two contribution reproduces the profile obtained from the complete Abelian Wilson loop. In other words, the AP-SU(2) flux-tube profile has the same detailed structure as that of the q - \bar{q} flux-tube solution in the DAH model.

The behavior of the profiles as a function of the q - \bar{q} distance r is also remarkable. While the monopole Wilson loop contributions, the solenoidal electric field and the monopole current profiles, are rather stable with respect to r , the photon Wilson loop contribution (*i.e.* the Coulombic electric field) drastically changes. From Fig. 4 it becomes obvious that the latter determines the change of the full Abelian electric field profile for different r . In order to see a really translationally invariant profile of the electric field, we need practically infinite q - \bar{q} separation, $r \rightarrow \infty$. In this limit, the profile only from the monopole part remains. This situation is, at least qualitatively, similar to the DAH model.

V. SUMMARY

It has already been known that the profiles of the classical flux-tube solution in the dual Abelian Higgs (DAH) model and of the Abelian-projected (AP) flux tube, observed in lattice simulations in the maximally Abelian gauge (MAG), look quite similar.

In this paper, in order to establish a more detailed correspondence between these two kinds of profiles, we have

studied the structure of both flux tubes more carefully. First, by applying the path-integral duality transformation to the Villain type compact QED considered as the approximate action of the AP gauge theory, we have been led to the construction of the U(1) DAH model. Along the way, we have identified the electric and magnetic parts of the Abelian Wilson loop by the Hodge decomposition. We have clarified the role of each contribution, the (electric) photon Wilson loop and the (magnetic) monopole Wilson loop, to the structure of the classical flux-tube solution in the DAH model. The profile of the electric field of the DAH flux tube consists of these two contributions, a Coulombic field associated with electric charges and a solenoidal field originating from the monopole supercurrent. Their superposition gives rise to a flux tube.

Guided by this observation, we have performed lattice simulations of the AP-SU(2) lattice gauge theory and have measured, in the MAG, the profiles induced by the photon and the monopole Wilson loops. We have found that the resulting profiles show the same structure as in the DAH flux tube: the superposition of a Coulombic electric field and a solenoidal electric field produces the AP flux tube.

The further question would be how both sides are related quantitatively. One way would be to fit the profile of the AP flux tube by that of the DAH flux tube, taking into account their sub-structures. This will provide the effective couplings of the DAH model. Such a quantitative analysis is in progress [45]. At the same time, it would also be important to understand why the AP flux tube and the DAH flux tube have this similar structure, although the former is created by full quantum effects, while the latter is just a classical solution. One natural answer could be that the path-integral duality transformation, the mapping $e \rightarrow g$, works very well and this would allow us indeed to deal with a weakly coupled infrared effective theory. The latter could be treated perturbatively on a quasi-classical level.

In closing, we note that although we have concentrated here on SU(2) gauge theory, the ideas discussed in the present paper can be extended to arbitrary AP-SU(N) gauge theory in the MAG [43, 46, 47].

Acknowledgments

We are grateful to V. Bornyakov, H. Ichie, G. Bali, R. W. Haymaker, D. Ebert, and M. N. Chernodub for useful discussions.

Y. K. was partially supported by the Ministry of Education, Science, Sports and Culture, Japan (Monbu-Kagaku-sho), Grant-in-Aid for Encouragement of Young Scientists (B), 14740161, 2002.

E.-M. I. acknowledges gratefully the support by Monbu-Kagaku-sho which allowed him to work within the COE program at Research Center for Nuclear Physics (RCNP), Osaka University, Japan. He expresses his personal thanks to H. Toki for the hospitality experienced at RCNP.

M. I. P. is partially supported by grants RFBR 02-02-17308, RFBR 01-02-117456, RFBR 00-15-96-786, INTAS-00-00111, and CRDF award RPI-2364-MO-02.

The computation was done on the Vector-Parallel Supercomputer NEC SX-5 at the RCNP, Osaka University, Japan.

APPENDIX A: LATTICE SIMULATION DETAIL

For the SU(2) link variables generated by Monte-Carlo method with Wilson gauge action, $U_\mu(s)$, we adopt the maximally Abelian gauge (MAG) fixing, which is achieved by maximizing the functional

$$R[U^V] = \sum_{s,\mu} \text{tr} \{ \tau_3 U_\mu^V(s) \tau_3 U_\mu^{V\dagger}(s) \} . \quad (\text{A1})$$

After the MAG fixing, Abelian projection is performed; the SU(2) link variables $U_\mu^V(s) = U_\mu^{MA}(s)$ are factorized into a diagonal (Abelian) link variable $u_\mu(s) \in \text{U}(1)_3$ and the off-diagonal (charged matter field) parts $c_\mu(s), c_\mu^*(s) \in \text{SU}(2)/\text{U}(1)_3$ as follows

$$U_\mu^{MA}(s) = \begin{pmatrix} \sqrt{1 - |c_\mu(s)|^2} & -c_\mu^*(s) \\ c_\mu^*(s) & \sqrt{1 - |c_\mu(s)|^2} \end{pmatrix} \begin{pmatrix} u_\mu(s) & 0 \\ 0 & u_\mu^*(s) \end{pmatrix} , \quad (\text{A2})$$

where the Abelian link variables $u_\mu(s)$ are then explicitly written as

$$u_\mu(s) = e^{i\theta_\mu(s)} \quad (\theta_\mu(s) \in [-\pi, \pi]) . \quad (\text{A3})$$

The Abelian plaquette variables is then constructed as

$$\theta_{\mu\nu}(s) \equiv \theta_\mu(s) + \theta_\nu(s + \hat{\mu}) - \theta_\mu(s + \hat{\nu}) - \theta_\nu(s) \in [-4\pi, 4\pi] , \quad (\text{A4})$$

which is decomposed into a regular part $\bar{\theta}_{\mu\nu}(s) \in [-\pi, \pi)$ and a singular (magnetic Dirac string) part $n_{\mu\nu}^{(m)}(s) = 0, \pm 1, \pm 2$ as follows

$$\theta_{\mu\nu}(s) \equiv \bar{\theta}_{\mu\nu}(s) + 2\pi n_{\mu\nu}^{(m)}(s) . \quad (\text{A5})$$

The Abelian field strength is defined by $\bar{\theta}_{\mu\nu}(s) = \theta_{\mu\nu}(s) - 2\pi n_{\mu\nu}^{(m)}(s)$. Following DeGrand and Touissaint [48], magnetic monopoles are extracted as the string boundaries

$$k_\mu(s_d) = -\frac{1}{2} \varepsilon_{\mu\nu\rho\sigma} \partial_\nu n_{\rho\sigma}^{(m)}(s + \hat{\mu}) \quad (\varepsilon_{1234} = 1) , \quad (\text{A6})$$

where $|k_\mu(s_d)| \leq 2$ and $s_d \equiv s + (\hat{1} + \hat{2} + \hat{3} + \hat{4})/2$ denotes the dual site.

For measuring the correlation function, we have used the following local operators: (i) an electric field operator

$$\mathcal{O}(s) = \bar{\theta}_{k4}(s) = \theta_{k4}(s) - 2\pi n_{k4}^{(m)}(s) , \quad (\text{A7})$$

and (ii) a monopole current operator

$$\mathcal{O}(s_d) = 2\pi k_l(s_d) \quad (l = i, j: \text{perpendicular to } k) . \quad (\text{A8})$$

The Abelian Wilson loop is constructed as

$$W_A[j] = \prod_{l \in j} u_\mu(s) = e^{i \sum_{l \in j} \theta_\mu(s)} . \quad (\text{A9})$$

Similarly, the photon and the monopole Wilson loop are constructed from the photon and monopole parts of Abelian link variables, θ^{ph} and θ^{mo} , respectively, where

$$\theta_\mu(s) = \Delta^{-1} \partial_\nu (\bar{\theta}_{\mu\nu}(s) + 2\pi n_{\mu\nu}^{(m)}(s)) = \theta_\mu^{ph}(s) + \theta_\mu^{mo}(s) . \quad (\text{A10})$$

In this decomposition, it is necessary to adopt the Abelian Landau gauge which is characterized by $\partial_\mu \theta_\mu(s) = 0$. Note, however, that the Wilson loops constructed from each link variable are Abelian gauge invariant.

In this simulation, in order to see the profiles which belong to the ground state of a flux tube, we have adopted a smearing technique for spacelike Abelian link variables. Then we have constructed the *smear*ed Abelian Wilson loop [38]. Considering the fourth direction as the Euclidean time direction, we have performed N_s times the following step in a smearing procedure applied only to the *spatial* Abelian links ($i, j = 1, 2, 3$),

$$\alpha e^{i\theta_i(s)} + \sum_{j \neq i} e^{i(\theta_j(s) + \theta_i(s+\hat{j}) - \theta_j(s+\hat{i}))} \rightarrow e^{i\theta_i(s)}, \quad (\text{A11})$$

where α is an appropriate smearing parameter. The same procedure was also applied to the spatial parts of the photon and the monopole link variables before constructing each type of Wilson loop.

The numerical simulations which are presented in this paper have been done at $\beta = 2.5115$. The lattice volume was 32^4 . We have used 100 configurations for measurements. We have produced them after 3000 thermalization sweeps, separated by 500 Monte Carlo updates. They have been stored for performing MAG fixing. This has been repeated N_g times, starting each time from a different random gauge copy of the configuration, in order to explore an increasing number of Gribov copies. The copy reaching the maximal value of the gauge functional (A1) has been selected for measuring the profiles and kept for further increasing of N_g . Finally we have chosen $N_g = 20$. For the MAG fixing itself, we have used the simulated annealing algorithm [38], followed by a final steepest descent relaxation. The size of the Wilson loops mainly studied (for Fig. 4, 5 and 6) are $R \times T = 6 \times 6$ and 12×6 in units of lattice spacing a . We have measured the profiles just on the midpoint of the Wilson loop. The Abelian smearing parameters have been found by optimization as $N_s = 8$ and $\alpha = 2.0$. With this choice, the profiles induced by the Abelian Wilson loop with timelike extensions $T = 8$ and $T = 6$ agree within errors.

The physical scale (the lattice spacing $a(\beta = 2.5115)$) has been determined from the non-Abelian string tension σ_L by fixing $\sqrt{\sigma_{phys}} = \sqrt{\sigma_L}/a \equiv 440$ MeV. The non-Abelian string tension has been re-evaluated by measuring expectation values of non-Abelian Wilson loops with an optimized non-Abelian smearing. The potential has been fitted to match the form $V(R) = C - A/R + \sigma_L R$. The resulting string tension is $\sigma_L = 0.0323(4)$ at $\beta = 2.5115$, such that the corresponding lattice spacing in physical units is $a(\beta) = 0.0806(5)$ fm.

-
- [1] G. 't Hooft, in *High-Energy Physics. Proceedings of the EPS International Conference, Palermo, Italy, 23-28 June 1975*, edited by A. Zichichi Vol. 2, pp. 1225–1249, Editrice Compositori, Bologna, 1976.
 - [2] S. Mandelstam, Phys. Rept. **23C**, 245 (1976).
 - [3] A. A. Abrikosov, Sov. Phys. JETP **5**, 1174 (1957).
 - [4] H. B. Nielsen and P. Olesen, Nucl. Phys. **B61**, 45 (1973).
 - [5] Y. Nambu, Phys. Rev. **D10**, 4262 (1974).
 - [6] M. Creutz, *Quarks, Gluons and Lattices* (Cambridge, Uk: Univ. Pr. (Cambridge Monographs on Mathematical Physics), 1983), 169p.
 - [7] K. Sailer, T. Schoenfeld, Z. Schram, A. Schaefer, and W. Greiner, J. Phys. **G17**, 1005 (1991).
 - [8] G. 't Hooft, Nucl. Phys. **B190**, 455 (1981).
 - [9] Z. F. Ezawa and A. Iwazaki, Phys. Rev. **D25**, 2681 (1982).
 - [10] Z. F. Ezawa and A. Iwazaki, Phys. Rev. **D26**, 631 (1982).
 - [11] T. Suzuki and I. Yotsuyanagi, Phys. Rev. **D42**, 4257 (1990).
 - [12] D. Zwanziger, Phys. Rev. **D3**, 880 (1971).
 - [13] K. Bardakci and S. Samuel, Phys. Rev. **D18**, 2849 (1978).
 - [14] T. Suzuki, Prog. Theor. Phys. **80**, 929 (1988).

- [15] S. Maedan and T. Suzuki, *Prog. Theor. Phys.* **81**, 229 (1989).
- [16] H. Suganuma, S. Sasaki, and H. Toki, *Nucl. Phys.* **B435**, 207 (1995), hep-ph/9312350.
- [17] S. Sasaki, H. Suganuma, and H. Toki, *Prog. Theor. Phys.* **94**, 373 (1995).
- [18] H. Shiba and T. Suzuki, *Phys. Lett.* **B343**, 315 (1995), hep-lat/9406010.
- [19] H. Shiba and T. Suzuki, *Phys. Lett.* **B351**, 519 (1995), hep-lat/9408004.
- [20] S. Kato, N. Nakamura, T. Suzuki, and S. Kitahara, *Nucl. Phys.* **B520**, 323 (1998).
- [21] M. N. Chernodub *et al.*, *Phys. Rev.* **D62**, 094506 (2000), hep-lat/0006025.
- [22] V. Singh, D. A. Browne, and R. W. Haymaker, *Phys. Lett.* **B306**, 115 (1993), hep-lat/9301004.
- [23] Y. Matsubara, S. Ejiri, and T. Suzuki, *Nucl. Phys. Proc. Suppl.* **34**, 176 (1994), hep-lat/9311061.
- [24] K. Bernstein, G. Di Cecio, and R. W. Haymaker, *Phys. Rev.* **D55**, 6730 (1997), hep-lat/9606018.
- [25] G. S. Bali, C. Schlichter, and K. Schilling, *Prog. Theor. Phys. Suppl.* **131**, 645 (1998), hep-lat/9802005.
- [26] F. V. Gubarev, E.-M. Ilgenfritz, M. I. Polikarpov, and T. Suzuki, *Phys. Lett.* **B468**, 134 (1999), hep-lat/9909099.
- [27] S. Kamizawa, Y. Matsubara, H. Shiba, and T. Suzuki, *Nucl. Phys.* **B389**, 563 (1993).
- [28] Y. Koma, H. Suganuma, and H. Toki, *Phys. Rev.* **D60**, 074024 (1999), hep-ph/9902441.
- [29] Y. Koma, E.-M. Ilgenfritz, T. Suzuki, and H. Toki, *Phys. Rev.* **D64**, 014015 (2001), hep-ph/0011165.
- [30] E. T. Akhmedov, M. N. Chernodub, M. I. Polikarpov, and M. A. Zubkov, *Phys. Rev.* **D53**, 2087 (1996), hep-th/9505070.
- [31] D. Antonov and D. Ebert, *Eur. Phys. J.* **C8**, 343 (1999), hep-th/9806153.
- [32] D. Antonov and D. Ebert, *Phys. Lett.* **B444**, 208 (1998), hep-th/9809018.
- [33] M. N. Chernodub and D. A. Komarov, *JETP Lett.* **68**, 117 (1998), hep-th/9809183.
- [34] Y. Koma, M. Koma, D. Ebert, and H. Toki, *JHEP* **08**, 047 (2002), hep-th/0108138.
- [35] Y. Koma, M. Koma, D. Ebert, and H. Toki, *Nucl. Phys.* **B648**, 189 (2003), hep-th/0206074.
- [36] J. D. Stack, S. D. Neiman, and R. J. Wensley, *Phys. Rev.* **D50**, 3399 (1994), hep-lat/9404014.
- [37] H. Shiba and T. Suzuki, *Phys. Lett.* **B333**, 461 (1994), hep-lat/9404015.
- [38] G. S. Bali, V. Bornyakov, M. Mueller-Preussker, and K. Schilling, *Phys. Rev.* **D54**, 2863 (1996), hep-lat/9603012.
- [39] T. Suzuki and M. N. Chernodub, Screening and confinement in $U(1)^{N-1}$ Abelian effective theories, 2002, hep-lat/0207018.
- [40] M. N. Chernodub and M. I. Polikarpov, Abelian projections and monopoles, 1997, hep-th/9710205.
- [41] Y. Koma, E.-M. Ilgenfritz, H. Toki, and T. Suzuki, *Phys. Rev.* **D64**, 011501 (2001), hep-ph/0103162.
- [42] Y. Koma and M. Koma, *Euro. Phys. J.* **C26**, 457 (2003), hep-ph/0109033,
- [43] Y. Koma, *Phys. Rev.* **D66**, 114006 (2002), hep-ph/0208066.
- [44] O. Miyamura, *Phys. Lett.* **B353**, 91 (1995).
- [45] Y. Koma, M. Koma, T. Suzuki, E.-M. Ilgenfritz, and M. I. Polikarpov, A fresh look on the flux tube in Abelian-projected $SU(2)$ gluodynamics, 2002, hep-lat/0210014.
- [46] V. Bornyakov *et al.*, *Nucl. Phys. Proc. Suppl.* **106**, 634 (2002), hep-lat/0111042.
- [47] H. Ichie, V. Bornyakov, T. Streuer, and G. Schierholz, The flux distribution of the three quark system in $SU(3)$, 2002, hep-lat/0212024.
- [48] T. A. DeGrand and D. Toussaint, *Phys. Rev.* **D22**, 2478 (1980).